J. Fluid Mech. (1974), *vol.* 64, *part* 1, *pp.* 1–16
Printed in Great Britain

On the development of dunes in erodible channels

By JØRGEN FREDSØE

Institute of Hydrodynamics and Hydraulic Engineering,
Technical University of Denmark, DK 2800 Lyngby/Copenhagen

(Received 2 February 1973 and in revised form 27 November 1973)

A two-dimensional stability analysis of the flow in a straight alluvial channel has been carried out, using the vorticity transport equation. In the analysis an attempt has been made to account for the influence of gravity on bed-load transport, and this turned out to change the stability quite significantly.

In the case of instability, the further growth of the dunes has been investigated using a second-order approximation. This nonlinear theory explains the experimental fact that the dunes very soon become asymmetric.

1. Introduction

Mathematical models describing the development of sand waves in alluvial streams, involving more or less realistic physical idealizations, have been suggested by several authors during the last decades. The first important step in recent years was made by Anderson (1953), who tried to explain the physical properties of fully developed sand waves by considering the flow of an ideal fluid over a sinusoidal bottom, assuming the sediment transport to be as bed load only.

Kennedy (1963) considered a two-dimensional potential flow over a sinusoidal bed, regarding the bed wave formation as a stability problem. In order to study instability he introduced the quantity δ, which is the distance by which the local sediment transport rate lags behind the local velocity at the bed. There is great uncertainty in connexion with the physical interpretation and evaluation of δ. Hayashi (1970) tried to reduce this uncertainty by considering the effect of the local bed inclination on the sediment transport.

Reynolds (1965) continued and extended Kennedy's theory and introduced a three-dimensional stability analysis. This was later investigated further by Engelund & Fredsøe (1971), still using potential-flow theory, but assuming a definite sediment transport model (suspension).

A physically reasonable model of the sediment transport was suggested in a paper by Engelund (1970). The model describes the two-dimensional flow of a real fluid by a vorticity transport equation and the transport of sediment in suspension by a diffusion equation. Engelund's theory explains physically the phase shift between the flow rate and the transport of sediment as being partly a result of the variation in the amount of sediment in suspension and partly a result of the fact that the friction itself introduces a phase shift between the bed form and the shear stress along the bottom.

The present paper may be regarded as a continuation of this work by Engelund. In the first sections, a linear stability analysis is carried out, the effect of the vorticity in the basic flow is discussed and the results are compared with previous results. The effect of the local bed inclination on the local rate of bed-load transport is taken into account. In the later sections, the growth of dunes in the unstable regions is investigated in order to obtain an explanation of the asymmetric growth.

Exner (1920, see Leliavsky 1955, p. 26) and Reynolds (1965) have explained this phenomenon by using a one-dimensional nonlinear flow model. In the present paper, the problem is considered from a different point of view. Using a second-order perturbation theory, the asymmetric distribution of the shear stress over a wavy bed is shown to cause the asymmetric form of the sand wave.

2. Analytical solution of the vorticity transport equation

The present analysis is mainly based on the equations suggested by Engelund (1970). The eddy viscosity ϵ is assumed to be constant and given by

$$\epsilon = 0{\cdot}077 U_{f0} D, \tag{1}$$

where D is the depth and U_{f0} is the friction velocity in the undisturbed flow, defined by

$$U_{f0} = (\tau_0/\rho)^{\frac{1}{2}}. \tag{2}$$

Here, τ_0 denotes the bed shear stress and ρ the fluid density.

Because of the assumption (1) it is necessary to introduce a fictitious slip velocity U_{b0} for the basic velocity profile U. This is found by matching the profile of the outer constant-stress layer with the correct velocity profile near the bottom. In Engelund's paper the outer solution was given by a parabola obtained by integration of the flow equations. To simplify the subsequent analysis, this parabola is replaced by a cosine:

$$U = U_{s0} \cos\{\beta(1 - x_2/D)\}, \tag{3}$$

where U_{s0} is the surface velocity, x_2 the co-ordinate perpendicular to the mean flow direction and β a constant. The velocity profile is shown in figure 1.

By putting

$$\beta^2 = 14 U_{f0}/U_{s0} \tag{4}$$

we obtain a very close numerical approximation to the parabola. The slip velocity U_{b0} at the bed is determined from (3):

$$U_{b0} = U_{s0} \cos\beta.$$

This slip velocity must satisfy the matching condition at the bed, which is

$$U_{b0}/U_{f0} = 1{\cdot}9 + 2{\cdot}5 \ln(D/k') = \kappa, \tag{5}$$

where k' is the equivalent sand roughness, suggested by Engelund (1970) to be $2{\cdot}5d$, where d is the diameter of the sediment grains.

The perturbed flow is described by the vorticity transport equation

$$d\omega/dt = \epsilon \nabla^2 \omega, \tag{6}$$

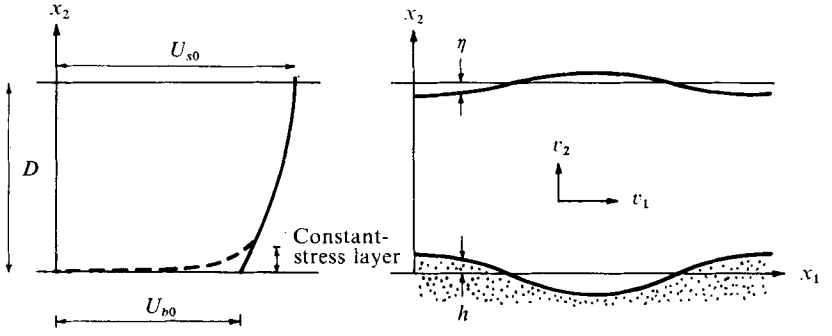

FIGURE 1. The velocity distribution in the uniform channel flow and definition sketch of the perturbed flow.

where the vorticity ω is defined by

$$2\omega = \partial v_2/\partial x_1 - \partial v_1/\partial x_2, \tag{7}$$

in which v_1 and v_2 are the velocity components and x_1 is the co-ordinate in the mean flow direction.

If the stream function ψ is defined by

$$v_1 = -\partial\psi/\partial x_2, \quad v_2 = \partial\psi/\partial x_1, \tag{8}$$

the vorticity is given by

$$\omega = \tfrac{1}{2}\nabla^2\psi. \tag{9}$$

Inserting (8) and (9) in (6) we get

$$-\frac{\partial\psi}{\partial x_2}\frac{\partial\nabla^2\psi}{\partial x_1} + \frac{\partial\psi}{\partial x_1}\frac{\partial\nabla^2\psi}{\partial x_2} + \frac{\partial\nabla^2\psi}{\partial t} = \epsilon\nabla^4\psi. \tag{10}$$

If the flow is assumed to be periodic, the perturbation h of the sand bed, the perturbation η of the surface and the perturbation $\tilde{\psi}$ of the flow can be written as

$$h = h_0 \exp\{ikD(\xi_1 - at/D)\}, \tag{11}$$

$$\eta = \eta_0 \exp\{ikD(\xi_1 - at/D)\}, \tag{12}$$

$$\tilde{\psi} = U_{b0} h_0 f(\xi_2) \exp\{ikD(\xi_1 - at/D)\}, \tag{13}$$

where h_0 and η_0 are the amplitudes of the perturbation of the bed and surface, respectively. kD is the dimensionless wavenumber, f is an unknown function, a is the complex migration velocity of the bed waves, $a = a_r + ia_i$, and $\xi_i = x_i/D$ are the dimensionless space variables.

By assuming the perturbation parameter h_0/D to be infinitely small, the linearized equation in f is obtained from (10):

$$f'' - (kD)^2 f - \frac{U''}{U} f = \frac{\epsilon}{(ikD^2U)} f^{\mathrm{iv}}, \tag{14}$$

preserving only the dominant term on the right-hand side and assuming that $|a| \ll U$. All the differentiations are with respect to ξ_2. Putting $\epsilon = 0$ in (14), the solution turns out to be

$$f = c_1 \exp\{\xi_2[(kD)^2 - \beta^2]^{\frac{1}{2}}\} + c_2 \exp\{-\xi_2[(kD)^2 - \beta^2]^{\frac{1}{2}}\}, \tag{15}$$

c_1 and c_2 being constants. This is the outer inviscid solution, which is seen to vary slowly with ξ_2. Since the inner frictional solution to (14) is of the boundary-layer type, i.e. rapidly damped, we may, on the right-hand side of (14), take $U = U_0$, where U_0 is a constant typical velocity in the interval $U_{b0} \leqslant U_0 \leqslant U_{s0}$. Now (14) is a linear differential equation with constant coefficients. The characteristic equation is

$$R^4 - \frac{ikD^2U_0}{\epsilon} R^2 + \frac{ikD^2U_0}{\epsilon}\{(kD)^2 - \beta^2\} = 0. \tag{16}$$

Next, we define

$$\epsilon^* = \epsilon/U_0 D = 0{\cdot}077 U_{f0}/U_0 \ll 1. \tag{17}$$

The roots of (16) are

$$\begin{aligned} R^2 &= \frac{ikD}{2\epsilon^*} \pm \left\{\left(\frac{ikD}{2\epsilon^*}\right)^2 - \frac{ikD}{\epsilon^*}[(kD)^2 - \beta^2]\right\}^{\frac{1}{2}} \\ &= \frac{ikD}{2\epsilon^*} \pm \frac{ikD}{2\epsilon^*}\left\{1 - \frac{2\epsilon^*}{ikD}[(kD)^2 - \beta^2]\right\} + O\left(\frac{\epsilon^*}{kD}\right) \\ &= \begin{cases} ikD/\epsilon^* + O(1), \\ (kD)^2 - \beta^2 + O(\epsilon^*/kD), \end{cases} \\ R &= \begin{cases} \pm (ikD/\epsilon^*)^{\frac{1}{2}} + O((\epsilon^*/kD)^{\frac{1}{2}}), \\ \pm [(kD)^2 - \beta^2]^{\frac{1}{2}} + O(\epsilon^*/kD). \end{cases} \end{aligned} \tag{18}$$

As long as $(\epsilon^*/kD)^{\frac{1}{2}} \ll 1$, the solution of (14) can be written as

$$\begin{aligned} f = c_1 \exp\{\xi_2[(kD)^2 - \beta^2]^{\frac{1}{2}}\} + c_2 \exp\{-\xi_2[(kD)^2 - \beta^2]^{\frac{1}{2}}\} \\ + c_3 \exp\{-\xi_2(ikD/\epsilon^*)^{\frac{1}{2}}\} + c_4 \exp\{\xi_2(ikD/\epsilon^*)^{\frac{1}{2}}\}, \end{aligned} \tag{19}$$

c_3 and c_4 being constants. The first two terms constitute the inviscid outer solution, as given by (15). The third term is damped very quickly away from the bed. Here, the value of U_0 has to be taken as U_{b0} in the definition of ϵ^*.

The last term is a frictional term, which is significant only in a small region close to the surface. Here, the value of U_0 is to be taken as U_{s0} in ϵ^*. As expected, this last term affects the flow only slightly. The following linear stability analysis has been carried out with and without this term with no difference in the results, so in the following this term is neglected in order to reduce the calculations.

3. Transport of sediment

Sediment is transported in two different ways, as bed load and in suspension. The rate q_b of bed-load transport is given by the relation (Meyer-Peter & Müller 1948)

$$\Phi_b = q_b/\{(s-1)gd^3\}^{\frac{1}{2}} = 8(\theta - 0{\cdot}047)^{\frac{3}{2}}, \tag{20}$$

where s denotes the relative density of the sediment grains, g the acceleration due to gravity and θ the Shields parameter, which can be written as

$$\theta = \tau d^2/(s-1)gd^3. \tag{21}$$

In this form, the parameter represents the ratio between the agitating and the stabilizing forces on a sediment grain in the bed. τ is the shear stress at the bottom, given by the expression

$$\tau/\rho = \epsilon(\partial v_1/\partial x_2 + \partial v_2/\partial x_1). \tag{22}$$

It should be mentioned here that the Meyer-Peter formula includes only shear stress due to the 'grain resistance'. In the case of a bottom which is only slightly perturbed, no drag resistance exists. Here, it is correct to use (22) in the definition of θ.

In the well-established relation (20), only the dynamic influence of the shear stress at the bottom is regarded as an agitating force. This is in accordance with the fact that the experiments from which this equation was obtained were carried out in a nearly horizontal flow. As shown experimentally by Lysne (1969), gravity is also a contributing factor to the grain force when the bed is sloping. In the analysis the effect of gravity is taken into account in the following way. The agitating shear force in the dimensionless Shields parameter is τd^2. When the bed is sloping, the additional gravity force component is given by μWI, where W is the submerged weight of the grains, I is the slope of the bed and μ a dynamic friction coefficient, $0 < \mu < 1$. The Shields parameter can now be written as

$$\theta^* = \frac{\tau d^2 + \mu(s-1)\,gd^3 I}{(s-1)\,gd^3} = \theta + \mu I. \tag{23}$$

In (23) the area and volume coefficients are included in the constant μ. Hence the order of μ must be about 0·1.

At low Froude numbers, the bed load is the dominating transport mechanism, and in this regime the dunes are formed. At higher flow rates where the antidunes develop, the sediment is increasingly transported in suspension. This has been taken into account in the present linear stability analysis, but for a detailed description the reader is referred to the paper by Engelund (1970) or to the paper by Engelund & Fredsøe (1971), where the suspension equations are solved analytically, using potential theory.

The total sediment load q_T is the sum of the bed load q_b and the suspended load q_s. For the total load we have the sediment continuity equation

$$\frac{\partial q_T}{\partial x_1} = -(1-n)\frac{\partial h}{\partial t} - \frac{\partial}{\partial t}\int_h^{D+\eta} c\,dx_2, \tag{24}$$

in which n is the porosity of the sand bed and c is the concentration of suspended sediment. The last term accounts for the sediment stored in suspension. In the case of bed load only, (24) reduces to

$$\partial q_b/\partial x_1 = -(1-n)\,\partial h/\partial t. \tag{25}$$

4. Boundary conditions

(i) The kinematic condition at the sand bed is

$$\frac{dh}{dt} = \frac{\partial h}{\partial t} + v_1\frac{\partial h}{\partial x_1} = v_2 \quad \text{at} \quad \xi_2 = \frac{h}{D}. \tag{26}$$

Within the framework of a linear theory and assuming that $|a| \ll U_b$, (26) gives

$$\frac{1}{U_{b0}}\frac{\partial \tilde{\psi}}{\partial x_1} = \frac{\partial h}{\partial x_1} \quad \text{at} \quad \xi_2 = 0. \tag{27}$$

(ii) The corresponding kinematic condition at the surface in the linear case is given by

$$\frac{1}{U_{s0}}\frac{\partial \tilde{\psi}}{\partial x_1} = \frac{\partial \eta}{\partial x_1} \quad \text{at} \quad \xi_2 = 1. \tag{28}$$

(iii) η may be eliminated from (28) by considering the dynamic boundary condition at the free surface. This condition states that the pressure at the surface is constant. Then, in the quasi-steady flow, the Bernoulli equation for the surface streamline is given by

$$\eta + (v_1^2 + v_2^2)/2g = \text{constant at } \xi_2 = 1 + \eta/D. \tag{29}$$

The linear form of (29), together with (28), gives

$$\tilde{\psi} = \mathscr{F}_s^2 \partial\tilde{\psi}/\partial\xi_2 \quad \text{at} \quad \xi_2 = 1, \tag{30}$$

where $\mathscr{F}_s$ is the Froude number based on the surface velocity: $\mathscr{F}_s = U_{s0}/(gD)^{\frac{1}{2}}$.

(iv) The last condition is related to the shear stress along the bed. The matching condition (5) is assumed also to be valid in the perturbed flow, i.e.

$$U_b/U_f = \kappa \quad \text{at} \quad \xi_2 = h/D. \tag{31}$$

U_f may be determined from (2) and (22), and the linear form of (31) then becomes

$$h\frac{dU}{dx_2} - \frac{\partial\tilde{\psi}}{\partial x_2} = \frac{\kappa^2\epsilon}{2U_{b0}}\left\{\frac{\partial^2\tilde{\psi}}{\partial x_1^2} - \frac{\partial^2\tilde{\psi}}{\partial x_2^2} + h\frac{d^2U}{dx_2^2}\right\} \quad \text{at} \quad \xi_2 = 0. \tag{32}$$

The constants c_1, c_2 and c_3 in (19) are determined from the three boundary conditions (27), (30) and (32). (As mentioned before, the last term in (19) is neglected.)

5. Linear stability analysis

Having obtained the function f, it is possible to carry out a stability analysis. The migration velocity a is found from (24). If the imaginary part a_i is positive, the perturbation will grow, indicating instability. For a_i negative, the perturbation will be attenuated, corresponding to a stable, plane bed. The value of a_i depends on the parameters $\mathscr{F}$, kD and V/U_{f0}, where V is the mean velocity and $\mathscr{F} = V/(gD)^{\frac{1}{2}}$ the Froude number based on the mean velocity.

For a constant value of V/U_{f0} it is possible to construct stability diagrams. Two such diagrams are shown in figure 2. In figure 2(*a*), the effect of gravity on the bed load is neglected. In figure 2(*b*), μ has the value 0·1. It is seen that only in the dune region are the stability limits changed significantly by the influence of gravity. This is in accordance with the fact that bed load is the dominating transport mechanism in the dunal regime, while the formation of antidunes is almost exclusively associated with sediment transported in suspension. The broken lines indicate the wavenumber which for a given Froude number has the largest growth rate, expressed by $kD \times a_i$.

Figure 3 shows the effect of changes in μ on the stability region. Again, the broken lines indicate the largest growth rates.

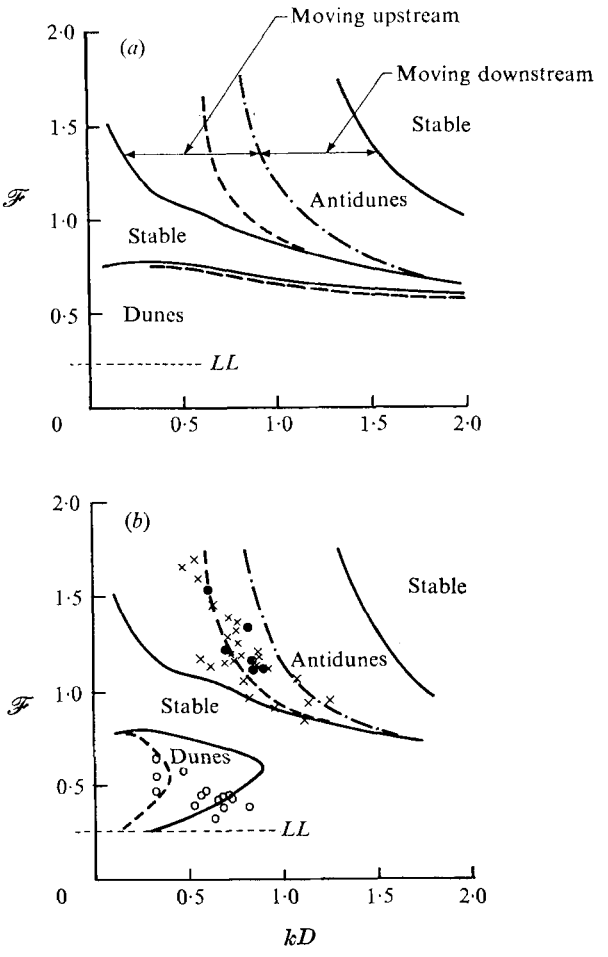

FIGURE 2. Stability diagrams. $V/U_{f0} = 20$. (*a*) $\mu = 0$. (*b*) $\mu = 0{\cdot}1$. Experiments by Guy *et al.* (1966): ×, antidunes; ●, standing waves; ○, dunes; *LL*, lower limit to sediment transport.

Unfortunately, it is difficult to compare the results from the stability analysis with observations in the dune region. The reason is that observations are made in the fully developed state, while the theory assumes a transient state. In the flow where the dunes are fully developed, the flow resistance is increased considerably compared with the plane bed situation. Hence, in natural streams, or in laboratory channels of the open-circuit type where the depth is free to vary, the depth increases, while the mean velocity and the Froude number decrease as the dune heights increase.

The best available data concerning mature dunes are the Fort Collins data (Guy, Simons & Richardson 1966). From the description of the operation procedure, it may be assumed that depth and discharge are kept constant during the growth, so that the Froude number remains constant. If it is assumed that the wavelength is preserved during the growth, kD also keeps its initial value. In fact, the wavelength may be increased a little during the growth, but as long as we

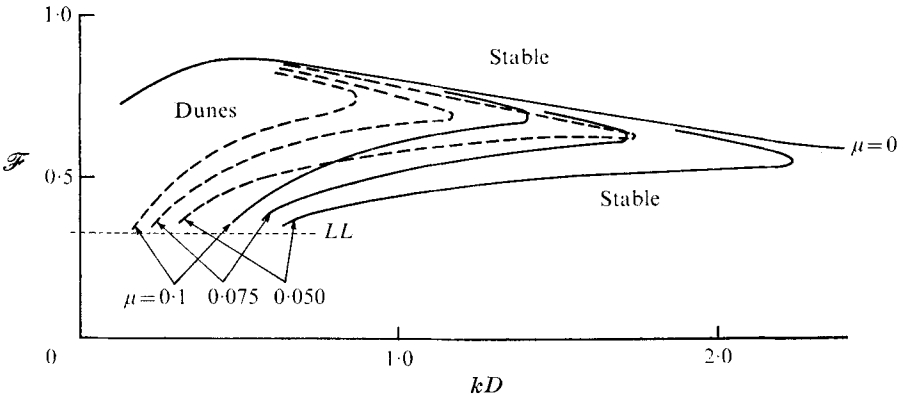

FIGURE 3. The stability region for dunes with different values of μ. $V/U_{f0} = 17$.

are concerned with dunes (as opposed to ripples), the assumption is acceptable. In figure 2, data for dunes are plotted for the grain sizes 0·27 mm and 0·28 mm. They fit reasonably well in the unstable region. It is seen that it is important to take the influence of gravity on the bed load into account. This explains the moderate value of kD, which is about 0·50 for the sand considered. If the effect of gravity is neglected, the stability analysis predicts the preferred wavenumber to be at least ten times greater (cf. figure 2*a*).

In the case of antidunes, the expansion loss is often negligible, and here the comparison with mature data should be expected to be better. In figure 2, data are plotted for sand with grain diameters between 0·19 and 0·47 mm (Guy *et al.* 1966). The results are within the unstable region and are close to the curve indicating the maximum growth rate.

In the case of coarser sand (0·93 mm), the mean value of kD in the dune region is about 0·9. This is in accordance with the theory, as seen in figure 4, where the stability regions for fine sand ($V/U_{f0} = 20$) and for coarser sand ($V/U_{f0} = 17$) are compared. The two curves are obtained from figure 2 ($V/U_{f0} = 20$) and figure 3 ($V/U_{f0} = 17$).

It should be noticed that the data for the ripples have been omitted above, because the formation of ripples is not covered by the present theory.

Finally, in this section the importance of the vorticity in the basic profile is investigated, partly because of the higher-order approximation used in the following sections. In figure 5 the stability limits in the dune region are shown, bed load being the only transport mechanism. μ is put equal to zero, only in order to isolate the influence of the flow on the bed. In fact, the use of a constant velocity profile (as was done by Engelund 1970) instead of the correct profile means only a very moderate change. The explanation is that it is the phase shift caused by the frictional term which is responsible for the instability of the bed in all cases where the sediment is transported mainly as bed load, and that the moderate variation of the basic velocity profile does not affect this phase shift significantly. The bottom velocity U_b is determined by the condition (5). As long as this boundary condition is maintained in the perturbed flow, the dynamic conditions close to the bed are still reasonably described.

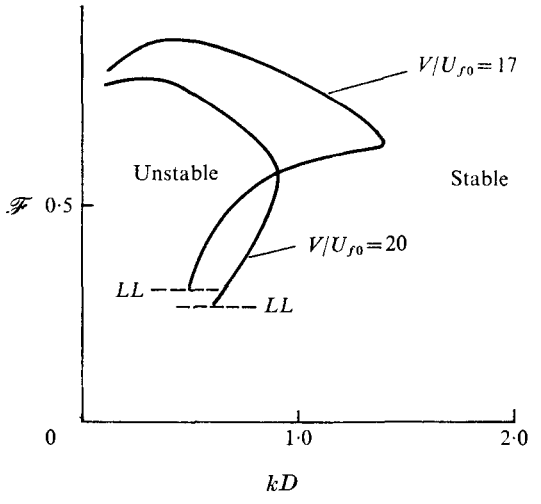

FIGURE 4. Changes in the stability regions with V/U_{f0}. The curves are taken from figures 2 and 3.

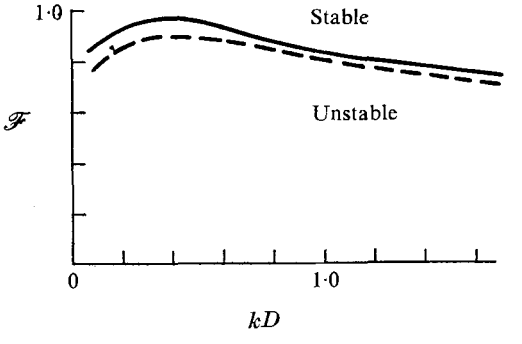

FIGURE 5. Comparison of stability limits in the dune region. $\mu = 0$. ——, constant basic velocity profile; – – – –, rotational basic velocity profile.

6. Second-order approximation

In the case of instability, the sand waves grow with time but in essentially different ways depending on whether the waves migrate as dunes or as antidunes. While antidunes when growing still have a regular symmetric sinusoidal bed form, the dunes rapidly obtained an asymmetric form, as was demonstrated experimentally by Raichlen & Kennedy (1965). As mentioned in the introduction, Exner (1920, see Leliavsky 1955, p. 26) and Reynolds (1965) have suggested this to be a nonlinear effect of a finite amplitude. Using a one-dimensional model Exner and Reynolds found that the velocity of the sand wave increases with the local height h of the sand wave, and further concluded that an originally symmetric wave after some time tends to be forward leaning.

In fact, Exner and Reynolds considered sand waves which are damped with time rather than growing, and their considerations are therefore not relevant in the present study. Further, it is possible to describe a symmetric sand wave which is travelling downstream without changing form by using a one-dimensional nonlinear flow model, in which the two-dimensional curvature effect of the flow pattern is taken into account (Engelund 1971). This suggests that, in order to give a reasonably accurate picture of the complicated nonlinear flow over a wavy bed, a two-dimensional flow description is needed.

The present model is an attempt to develop such a two-dimensional description to the second order of approximation. The asymmetric growth is found to be caused by the phase shift between the erosion and the mean velocity. This phase shift also explains why not all disturbances in the linear stability analysis are neutral.

As we are interested in the growth of dunes, the sediment is assumed to be transported as bed load only. Hence, the phase shift between erosion and mean velocity is caused by the internal friction of the fluid.

The calculation of the asymmetric growth is performed by extending the linear theory described in the first sections to a second-order approximation. The perturbation of the sand bed is still assumed to be very small. The changes in the bed shear-stress distribution caused by an arbitrary perturbation $h(x_1, t)$ of the bottom are found and using the fundamental sediment continuity equation (25) (bed load being the only transport mechanism) the form of the sand wave h is related to the shear-stress distribution caused by the perturbation h. In this way, it is possible to calculate the form of h, taking into account the fact that the wave is travelling downstream with a velocity a_r and growing with time.

The rotation of the basic profile (3) is neglected. This is done to simplify the analysis and the numerical calculations, whose details, in a higher-order approximation, often tend to hide the general trend. The assumption is justified in § 5. Equation (3) can now be written as

$$\psi = -Vx_2. \tag{33}$$

Now, we assume that, as long as the perturbation is small, the boundary conditions and the nonlinear vorticity transport equation can be expressed as power series in γ, which is the amplitude in the linearized problem,

$$\gamma = h_0/D, \tag{34}$$

i.e.

$$\left.\begin{aligned} h &= \gamma h_{(1)} + \gamma^2 h_{(2)} + \gamma^3 h_{(3)} + \ldots, \\ \eta &= \gamma \eta_{(1)} + \gamma^2 \eta_{(2)} + \gamma^3 \eta_{(3)} + \ldots, \end{aligned}\right\} \tag{35}$$

and

$$\psi = \psi_{(0)} + \gamma\psi_{(1)} + \gamma^2\psi_{(2)} + \ldots. \tag{36}$$

Here, $\gamma h_{(1)}$ is the same term as h in (11), i.e.

$$h_{(1)} = \cos\{kD(\xi_1 - a_r t/D)\} \exp(kDa_i t/D), \tag{37}$$

and similarly $\psi_{(0)}$ corresponds to (33) and $\psi_{(1)}$ to (13), which can be expanded into the real form necessary in the higher-order theory to yield

$$\begin{aligned}\psi_{(1)} = {} & VD\{c_1\exp(kD\xi_2)+c_2\exp(-kD\xi_2)\}\cos\{kD(\xi_1-a_rt/D)\}\exp(kDa_it/D)\\ & + VD\{d_1\exp(kD\xi_2)+d_2\exp(-kD\xi_2)\}\sin\{kD(\xi_1-a_rt/D)\}\exp(kDa_it/D)\\ & + VDc_3\exp\left\{-\left(\frac{kD}{2\epsilon^*}\right)^{\frac{1}{2}}\xi_2\right\}\cos\left\{-\left(\frac{kD}{2\epsilon^*}\right)^{\frac{1}{2}}\xi_2+kD(\xi_1-a_rt/D)\right\}\exp(kDa_it/D)\\ & + VDd_3\exp\left\{-\left(\frac{kD}{2\epsilon^*}\right)^{\frac{1}{2}}\xi_2\right\}\sin\left\{-\left(\frac{kD}{2\epsilon^*}\right)^{\frac{1}{2}}\xi_2+kD(\xi_1-a_rt/D)\right\}\exp(kDa_it/D).\end{aligned} \tag{38}$$

The development of (35) and (36) is a normal regular perturbation problem. To be correct, it is also necessary to develop the migration velocity a_r and the growth rate a_i, which depend on the parameters kD, $\mathscr{F}$ and V/U_{f0}. As in normal Stokes waves, changes in a_r and a_i will only take place in a third-order approximation.

The definition (17) of ϵ^* is given by

$$\epsilon^* = 0{\cdot}077U_{f0}/V, \tag{39}$$

and now the replacement of U by U_{b0} in (18) is not an approximation. Thereby, the error in determining the root of the friction term is $O((\epsilon^*/kD)^{\frac{1}{2}})$, compared with that in (18).

7. Second-order flow equation, boundary conditions and sediment continuity equation

The second-order flow equation is found by inserting (38) in the complete vorticity transport equation (10) and comparing the coefficient with γ^2. We get the following inhomogeneous differential equation:

$$\begin{aligned}-\frac{\partial\psi_{(0)}}{\partial x_2}\frac{\partial}{\partial x_1}(\nabla^2\psi_{(2)})+\frac{\partial}{\partial x_2}(\nabla^2\psi_{(0)})\frac{\partial\psi_{(2)}}{\partial x_1}+\frac{\partial}{\partial t}(\nabla^2\psi_{(2)})-\epsilon\nabla^4\psi_{(2)}\\ =\frac{\partial\psi_{(1)}}{\partial x_2}\frac{\partial}{\partial x_1}(\nabla^2\psi_{(1)})-\frac{\partial\psi_{(1)}}{\partial x_1}\frac{\partial}{\partial x_2}(\nabla^2\psi_{(1)})=I_E.\end{aligned} \tag{40}$$

In the same way, the second-order boundary conditions have been found. The kinematic condition at the bottom is

$$\frac{\partial\psi'_{(2)}}{\partial\xi_1}-\frac{\partial h'_{(2)}}{\partial\xi_1}=-h'_{(1)}\frac{\partial^2\psi'_{(1)}}{\partial\xi_1\partial\xi_2}-\frac{\partial\psi'_{(1)}}{\partial\xi_2}\frac{\partial h'_{(1)}}{\partial\xi_1}\quad\text{at}\quad\xi_2=0, \tag{41}$$

in which the following abbreviations have been introduced:

$$h'_{(1)}=h_{(1)}/D,\quad\psi'_{(1)}=\psi_{(1)}/VD,\quad\psi'_{(2)}=\psi_{(2)}/VD.$$

The boundary condition equivalent to (30), which is a combination of the kinematic condition and the dynamic Bernoulli equation at the surface, is

$$\frac{\partial \psi'_{(2)}}{\partial \xi_1} - \mathscr{F}^2 \frac{\partial^2 \psi'_{(2)}}{\partial \xi_1 \partial \xi_2} = \mathscr{F}^4 \frac{\partial}{\partial \xi_1}\left\{\frac{\partial \psi'_{(1)}}{\partial \xi_2}\frac{\partial^2 \psi_{(1)}}{\partial \xi_2^2}\right\} - 2\mathscr{F}^2 \frac{\partial \psi'_{(1)}}{\partial \xi_2}\frac{\partial^2 \psi'_{(1)}}{\partial \xi_1 \partial \xi_2} - \frac{\mathscr{F}^2}{2}\frac{\partial}{\partial \xi_1}\left\{\left[\frac{\partial \psi'_{(1)}}{\partial \xi_1}\right]^2 + \left[\frac{\partial \psi'_{(1)}}{\partial \xi_2}\right]^2\right\} \quad \text{at} \quad \xi_2 = 1. \tag{42}$$

The last boundary condition of the second-order approximation is obtained from (31). The condition equivalent to (32) is

$$-\frac{\partial \psi'_{(2)}}{\partial \xi_2} - \frac{\kappa^2 \epsilon}{2VD}\left\{\frac{\partial^2 \psi'_{(2)}}{\partial \xi_1^2} - \frac{\partial^2 \psi'_{(2)}}{\partial \xi_2^2}\right\} = -\frac{1}{2}\left\{\frac{\partial \psi'_{(1)}}{\partial \xi_1}\right\}^2 - \frac{1}{2}\left\{\frac{\partial \psi'_{(1)}}{\partial \xi_2}\right\}^2 + h'_{(1)}\frac{\partial^2 \psi'_{(1)}}{\partial \xi_2^2} + \frac{\kappa^2 \epsilon}{2VD}\left\{h'_{(1)}\frac{\partial^3 \psi'_{(1)}}{\partial \xi_1^2 \partial \xi_2} - h'_{(1)}\frac{\partial^3 \psi'_{(1)}}{\partial \xi_2^3} + \frac{\partial h'_{(1)}}{\partial \xi_1}\frac{\partial^2 \psi'_{(1)}}{\partial \xi_1 \partial \xi_2}\right\} \quad \text{at} \quad \xi_2 = 0. \tag{43}$$

All the inhomogeneities in the differential equation (40) and the boundary equations (41), (42) and (43) are products of terms of the form

$$f_1(\xi_2)\cos\{kD(\xi_1 - a_r t/D)\}\exp(ka_i t)$$

or

$$f_2(\xi_2)\sin\{kD(\xi_1 - a_r t/D)\}\exp(ka_i t).$$

By multiplying such terms by each other, products of the form

$$f_3(\xi_2)\cos\{2kD(\xi_1 - a_r t/D)\}\exp(2ka_i t),$$

$$f_4(\xi_2)\sin\{2kD(\xi_1 - a_r t/D)\}\exp(2ka_i t)$$

or

$$f_5(\xi_2)$$

are obtained.

In order to produce these inhomogeneities, it is seen that the second-order wave $h_{(2)}$ must migrate downstream at the same velocity a_r as the first-order wave $h_{(1)}$, its wavenumber being, however, twice that of the first-order wave. Furthermore, it must grow exponentially with an amplification factor twice that of the first-order wave, i.e.

$$h_{(2)} = [h_1\cos\{2kD(\xi_1 - a_r t/D)\} + h_2\sin\{2kD(\xi_1 - a_r t/D\} + h_3]\exp(2kDa_i t/D),$$

h_1, h_2 and h_3 being constants.

If the definition (34) of γ is changed to

$$\gamma = (h_0/D)\exp(kDa_i t/D)$$

all the growth with time is now contained in the development parameter, and it is seen that the influence of the higher-order terms increases with time. Since it is assumed that the perturbation of the bed is small, $\gamma \ll 1$, it is seen that the present theory is valid only at small values of $ka_i t$, when the first-order terms dominate the higher-order terms.

Finally, the sediment continuity equation (25) (bed load being the only transport mechanism) must be satisfied for all values of γ. As mentioned already, the

migration velocity and the growth velocity are found from the first-order approximation and are not changed in a second-order approximation. The real first-order form of (25) is

$$(1-n)\{a_r\,\partial h_{(1)}/\partial x_1 - ka_i h_{(1)}\} = \partial q_{b(1)}/\partial x_1. \tag{44}$$

In the same way, the second-order form turns out to be

$$(1-n)\{a_r\,\partial h_{(2)}/\partial x_1 - 2ka_i h_{(2)}\} = \partial q_{b(2)}/\partial x_1. \tag{45}$$

$q_{b(1)}$ and $q_{b(2)}$ are found from (20). θ, defined by (21), is written, using (2), as

$$\theta = \frac{U_f^2}{(s-1)gd} = \frac{D}{d}\left(\frac{U_f}{U_b}\right)^2 \frac{\mathscr{F}^2}{s-1}\left(\frac{U_b}{V}\right)^2. \tag{46}$$

Here, the quantity

$$\mathscr{H} = \frac{D}{d}\left(\frac{U_f}{U_b}\right)^2 \frac{\mathscr{F}^2}{s-1}$$

is not changed in the perturbed flow, while the local value of U_b must be inserted in (46). Now, (20) gives

$$\frac{q_b}{8\{(s-1)\,d^3\}^{\frac{1}{2}}} = \left\{\mathscr{H}\left(\frac{U_b}{V}\right)^2 - 0{\cdot}047 - \mu\frac{\partial h}{\partial x_1}\right\}^{\frac{3}{2}}. \tag{47}$$

Comparing the coefficients of γ^0 in (47), we get

$$q_{b(0)} = (\mathscr{H} - 0{\cdot}047 + \mu I_0)^{\frac{3}{2}}\, 8\{(s-1)\,d^3\}^{\frac{1}{2}},$$

in which I_0 in the unperturbed flow is given by

$$I_0 = (U_{f0}/V)^2\,\mathscr{F}^2.$$

Comparing the coefficients of γ^1 and of γ^2, we obtain

$$\frac{q_{b(1)}}{q_{b(0)}} = \frac{3}{2(\mathscr{H} - 0{\cdot}047 + \mu I_0)}\left\{-2\mathscr{H}\frac{\partial \psi'_{(1)}}{\partial \xi_2} - \mu\frac{\partial h'_{(1)}}{\partial \xi_1}\right\} \quad \text{at} \quad \xi_2 = 0, \tag{48}$$

and

$$\frac{q_{b(2)}}{q_{b(0)}} = \frac{3}{2(\mathscr{H} - 0{\cdot}047 + \mu I_0)}\left\{-2\mathscr{H}\frac{\partial \psi'_{(2)}}{\partial \xi_2} - \mu\frac{\partial h'_{(2)}}{\partial \xi_1} - 2\mathscr{H}h'_{(1)}\frac{\partial^2 \psi'_{(1)}}{\partial \xi_2^2} + \mathscr{H}\left[\frac{\partial \psi'_{(1)}}{\partial \xi_2}\right]^2 + \mathscr{H}\left[\frac{\partial \psi'_{(1)}}{\partial \xi_1}\right]^2\right\} + \frac{3}{8}\frac{[2\mathscr{H}\,\partial \psi'_{(1)}/\partial \xi_2 + \mu\,\partial h'_{(1)}/\partial \xi_1]^2}{\mathscr{H} - 0{\cdot}047 + \mu I_0} \quad \text{at} \quad \xi_2 = 0. \tag{49}$$

Together with (45), (49) gives the second-order continuity equation for the sediment.

8. Solutions

The flow equation (40) is solved in the same way as (10). The complete solution consists of the particular solution to the inhomogeneous equation and the solutions to the homogeneous equation.

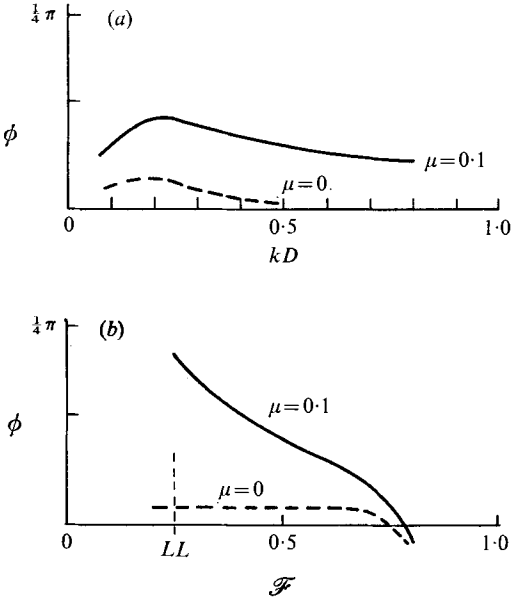

FIGURE 6. The variation of ϕ with (*a*) kD ($\mathscr{F} = 0{\cdot}5$) and (*b*) $\mathscr{F}$ ($kD = 0{\cdot}3$). $V/U_{f0} = 20$.

The inhomogeneous term on the right-hand side of (40) turns out to be

$$\begin{aligned} I_E = {} & \alpha_1 \exp\{[kD - (kD/2\epsilon^*)^{\frac{1}{2}}]\,\xi_2\} \cos\{2kD(\xi_1 - a_r t/D) - (kD/2\epsilon^*)^{\frac{1}{2}}\,\xi_2\} \\ & + \alpha_2 \exp\{[kD - (kD/2\epsilon^*)^{\frac{1}{2}}]\,\xi_2\} \sin\{2kD(\xi_1 - a_r t/D) - (kD/2\epsilon^*)^{\frac{1}{2}}\,\xi_2\} \\ & + \alpha_3 \exp\{[-kD - (kD/2\epsilon^*)^{\frac{1}{2}}]\,\xi_2\} \cos\{2kD(\xi_1 - a_r t/D) - (kD/2\epsilon^*)^{\frac{1}{2}}\,\xi_2\} \\ & + \alpha_4 \exp\{[-kD - (kD/2\epsilon^*)^{\frac{1}{2}}]\,\xi_2\} \sin\{2kD(\xi_1 - a_r t/D) - (kD/2\epsilon^*)^{\frac{1}{2}}\,\xi_2\} + \alpha_5, \end{aligned} \tag{50}$$

where the coefficients α_1, α_2, α_3, α_4 and α_5 are determined by insertion in (40). The particular solution $\psi_{(2)p}$ is of exactly the same form as I_E and is easily found. The solution to the homogeneous part of (40) has the following form:

$$\begin{aligned} \psi_{(2)h} = {} & VD\{e_1 \exp(2kD\xi_2) + e_2 \exp(-2kD\xi_2)\} \cos\{2kD(\xi_1 - a_r t/D)\} \\ & + VD\{f_1 \exp(2kD\xi_2) + f_2 \exp(-2kD\xi_2)\} \sin\{2kD(\xi_1 - a_r t/D)\} \\ & + VDe_3 \exp\{-(kD/\epsilon^*)^{\frac{1}{2}}\,\xi_2\} \cos\{+(kD/\epsilon^*)^{\frac{1}{2}}\,\xi_2 + 2kD(\xi_1 - a_r t/D)\} \\ & + VDf_3 \exp\{-(kD/\epsilon^*)^{\frac{1}{2}}\,\xi_2\} \sin\{-(kD/\epsilon^*)\,\xi_2 + 2kD(\xi_1 - a_r t/D)\}, \end{aligned} \tag{51}$$

e_1, e_2, e_3, f_1, f_2 and f_3 being constants.

By inserting the total solution for $\psi_{(2)}$ and the expression for $h_{(2)}$ in the three boundary conditions, (41), (42) and (43), and the second-order continuity equation for the sediment and comparing the coefficients of $\cos\{2kD(\xi_1 - a_r t/D)\}$

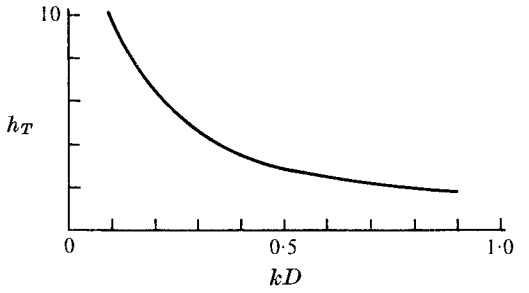

FIGURE 7. The variation of h_T with kD. $\mathscr{F} = 0{\cdot}3$ and $V/U_{f0} = 20$.

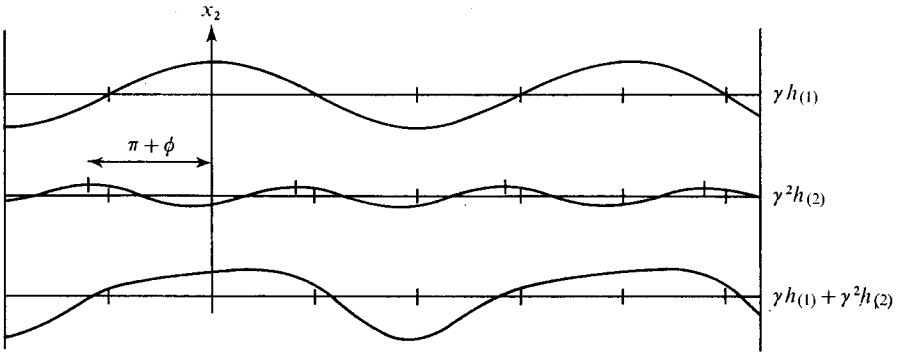

FIGURE 8. The sum of the first- and second-order waves. $\phi = \frac{1}{6}\pi$.

and of $\sin\{2kD(\xi_1 - a_r t/D)\}$, we obtain eight linear inhomogeneous equations in $e_1, e_2, e_3, f_1, f_2, f_3, h_1$ and h_2.

It is also possible to determine h_3 by comparing the constants in the boundary conditions, but this is of no interest in this connexion.

By re-writing $h_{(2)}$ as

$$h_{(2)} = h_T \cos\{2kD(\xi_1 + \pi + \phi - a_r t/D)\} + h_3,$$

where $\tan\phi = h_2/h_1$ and $h_T = (h_1^2 + h_2^2)^{\frac{1}{2}}$, it is easy to illustrate the asymmetric development of the dunes. In figure 6, the variation of ϕ with the wavenumber and the Froude number is shown. In the entire region of interest, ϕ always turns out to be a positive quantity, i.e. the sum of the first- and second-order waves is steeper downstream than upstream of the crest; see figure 8. Although the wave is also asymmetric when the influence of the gravity on the bed load is neglected, the obliquity increases considerably when this influence is taken into account.

In figure 7, the variation in h_T with kD is shown. This quantity is not of any great interest, because it is changing with time. However, it indicates how quickly the asymmetry increases. The value of h_T is moderate. It might be expected to be very large because of the large friction gradient at the bottom. In the boundary conditions, this large gradient is almost cancelled out by the particular solution $\psi_{(2)p}$, which explains the moderate value of h_T.

In figure 8, an example of an asymmetric wave is shown; $h \sim \gamma h_{(1)} + \gamma^2 h_{(2)}$. ϕ has the value $\frac{1}{6}\pi$, which for instance is the case if the Froude number is equal to 0·3,

V/U_{f0} equal to 20 and kD equal to 0·3; see figure 6. This composition of $\mathscr{F}$, kD and V/U_{f0} is in agreement with the maximum growth rate of dunes; see figure 2.

As a closing remark on the second-order approximation, it should be mentioned that, if the internal friction of the fluid is neglected, $h_{(2)}$ turns out to be zero, corresponding to the velocity at the bottom and the mean velocity being in phase. That is, if the internal friction is neglected, a symmetric wave is the only possible solution in the second-order approximation.

9. Conclusion

In the linear stability analysis, it is shown that the influence of gravity plays an important role with respect to the formation of dunes. In a further, second-order approximation, the phase shift between the erosion and the mean velocity caused by the internal friction of fluid explains why the dunes develop asymmetrically.

This article forms part of the author's Ph.D. study under the supervision of F. A. Engelund, to whom the author is grateful for stimulating discussions.

REFERENCES

ANDERSON, A. G. 1953 The characteristics of sediment waves formed by flow in open channels. *Proc. 3rd Midwestern Conf. on Fluid Mech., University of Minnesota, Minneapolis*, pp. 379–395.

ENGELUND, F. 1970 Instability of erodible beds. *J. Fluid Mech.* **42**, 225–244.

ENGELUND, F. 1971 The solitary sand wave (part I). *Prog. Rep. Inst. Hydrodyn. & Hydraul. Engng, Tech. University of Denmark*, no. 24, pp. 51–54.

ENGELUND, F. & FREDSØE, J. 1971 Three-dimensional stability analysis of open channel flow over an erodible bed. *Nordic Hydrology*, **2**, 93–108.

GUY, H. P., SIMONS, D. B. & RICHARDSON, E. V. 1966 Summary of alluvial channel data from flume experiments. 1956–61. *Geol. Survey Prof. Paper*, no. 462-I, pp. 1–96.

HAYASHI, T. 1970 Formation of dunes and antidunes in open channels. *Proc. A.S.C.E.* **96** (HY 2), 357–366.

KENNEDY, J. F. 1963 The mechanics of dunes and antidunes in erodible bed channels. *J. Fluid Mech.* **16**, 521–544.

LELIAVSKY, S. 1955 *An Introduction to Fluid Hydraulics*. London: Constable.

LYSNE, D. K. 1969 Movement of sand in tunnels. *Proc. A.S.C.E.* **95**, 1835–1846.

MEYER-PETER, E. & MÜLLER, R. 1948 Formulas for bed-load transport. *IAHSR, Rep. on 2nd Meeting*, vol. 3, pp. 39–64.

RAICHLEN, F. & KENNEDY, J. F. 1965 The growth of sediment bed forms from an initially flattened bed. *IAHR Congr., Leningrad*, paper no. 37.

REYNOLDS, A. J. 1965 Waves on the erodible bed of an open channel. *J. Fluid Mech.* **22**, 113–133.